A Mumford-Shah Functional based Variational Model with Contour, Shape, and Probability Prior information for Prostate Segmentation

Soumya Ghose, Jhimli Mitra, Arnau Oliver, Robert Marti, Xavier Llado, Jordi Freixenet, Joan C. Vilanova, Josep Comet, Désiré Sidibé, Fabrice Mériaudeau

A Mumford-Shah Functional based Variational Model with Contour, Shape, and Probability Prior information for Prostate Segmentation

S. Ghose[1,2], J. Mitra[1,2], A. Oliver[2], R. Martí[2], X. Lladó[2], J. Freixenet[2],
J. C. Vilanova[3], J. Comet[4], D. Sidibé[1], and F. Meriaudeau[1]
[1] *Univ. de Bourgogne, France,* [2] *Univ. de Girona, Spain,*
[3] *Girona Magnetic Resonance Center, Spain,* [4]*University Hospital Dr. Josep Trueta, Girona, Spain.*
(jhimli.mitra/soumya.ghose/dro-desire.sidibe/fmeriau)@u-bourgogne.fr, (marly/llado/aoliver)@eia.udg.edu

Abstract

Inter patient shape, size and intensity variations of the prostate in transrectal ultrasound (TRUS) images challenge automatic segmentation of the prostate. In this paper we propose a variational model driven by Mumford-Shah (MS) functional for segmenting the prostate. Parametric representation of the implicit curve is derived from principal component analysis (PCA) of the signed distance representation of the labeled training data to impose shape prior. Posterior probability of the prostate region determined from random forest classification facilitates initialization and propagation of our model in a MS energy minimization framework. The proposed method achieves mean Dice similarity coefficient (DSC) value of 0.97±0.01, with a mean Hausdorff distance (HD) value of 1.73±0.24 mm when validated with 24 images from 6 datasets in a leave-one-patient-out validation framework. The model achieves statistically significant t-test p-value<0.0001 in mean DSC and mean HD values compared to traditional statistical models of shape and appearance.

1. Introduction

Prostate volume determined from segmented TRUS images serves as an important parameter in determining presence of benign or malignant tumor during diagnosis of prostate diseases. Segmented 2D axial mid gland slices in TRUS images are used to estimate prostate volume using planimetry calculation, prolate ellipse volume calculation, and ellipsoid volume measurement [6]. However, accurate automatic or semi-automatic computer aided prostate segmentation from TRUS images is a challenging task due to low contrast of TRUS images, speckle and shadow artifacts, inter-patient prostate shape, size and deformation variations and heterogeneous intensity distribution inside the prostate gland. To deal with these challenges we propose a MS functional [10] based variational framework to segment the prostate. Implicit shape prior of the parametric curve is derived from PCA of the signed distance functions (SDFs) of the labeled training images. Posterior probabilities of the prostate region derived in a supervised learning framework of random forest is used in initialization and evolution of the parametric curve. The parameters of the evolving curve are determined from minimization of region and contour based energy as proposed in [1]. Quantitative comparison of our proposed method with the traditional AAM [4] and also with [9, 8] shows statistically significant improvement in overlap and contour accuracies. The key contributions of this work are; (1) The use of a random forest framework to obtain a soft classification of the prostate. (2) The use of shape, contour and probability prior information for evolution of levelsets. The remaining paper is organized in the following manner. Section 2 provides a description of the proposed segmentation framework, followed by the results and discussions in Section 3. Finally, the paper concludes in Section 4.

2. Proposed Segmentation Framework

The proposed method is developed on two major components: 2.1) supervised learning framework of random forest to determine posterior probability of a pixel being prostate, and 2.2) adapting implicit shape, boundary and intensity prior model of [1] to incorporate the posterior probabilities of the prostate region for initialization and evolution of the implicit curve.

2.1 Random forest based classification

In TRUS images prostate region have a heterogeneous intensity distribution and depending on the acquisition parameters the region based statics (mean and standard deviation) of the prostate may not significantly

vary from the background. Moreover, shadow artifacts and speckle may adversely affect the region based statistics (determined from intensities) of the prostate and the background. Significant separation of the intensities of the prostate and the background is essential for MS energy minimization framework. Moreover, inaccurate region based statistics of the prostate and the background adversely affect levelsets propagation and hence segmentation accuracies. Therefore, to reduce intensity variations inside the prostate region, and significantly separate the intensities of the prostate and the background we propose to determine the posterior probability of the image pixels being prostate in a supervised learning framework of random forest and substitute intensities with probabilities to achieve a better representation of the prostate and the background. Decision trees are discriminative classifiers which are known to suffer from over-fitting. However, a random decision forest or random forest achieves better generalization by growing an ensemble of many independent decision trees on a random subset of the training data and by randomizing the features made available at each node during training [2].

During **training**, rigidly alignment of the training datasets ensures minimization of pose variations. Similarly, inter-patient intensity variations are normalized. The data consists of a collection of $V = (X, F)$, each centered at 3×3 neighborhood of pixels. Where, $X = (x, y)$ denotes the pixel position and the feature vector F constitutes of the mean and standard deviation of the 3×3 pixel neighborhood. Each tree τ_i in random forest receives the full set V, along with the label and the root node and selects a test to split V into two subsets to maximize the information gain. A test constitutes of a feature (like the mean of a pixel neighborhood) and a feature response threshold. The left and the right child nodes receive their respective subsets of V and the process is repeated at each child node to grow the next level of the tree. Growth is terminated when either the information gain is minimum or the tree has grown to a maximum depth specified. Each decision tree in the forest is unique as each tree node selects a random subset of features and threshold. During **testing**, the test image is rigidly aligned to the same frame of the training datasets and its intensities are normalized. The pixels are routed to one leaf in each tree by applying the test (selected during training). Each pixel of the test dataset is propagated through all the trees by successive application of the relevant binary test to determine the probability of belonging to class c. When reaching a leaf node l_τ, where $\tau \in [1..., \Gamma]$, the posterior probabilities ($P_\tau(c|V)$) are gathered in order to compute the final posterior probability of the pixel defined by $P(c|V) = \frac{1}{\Gamma} \sum_{\tau=1}^{\Gamma} P_\tau(c|V)$.

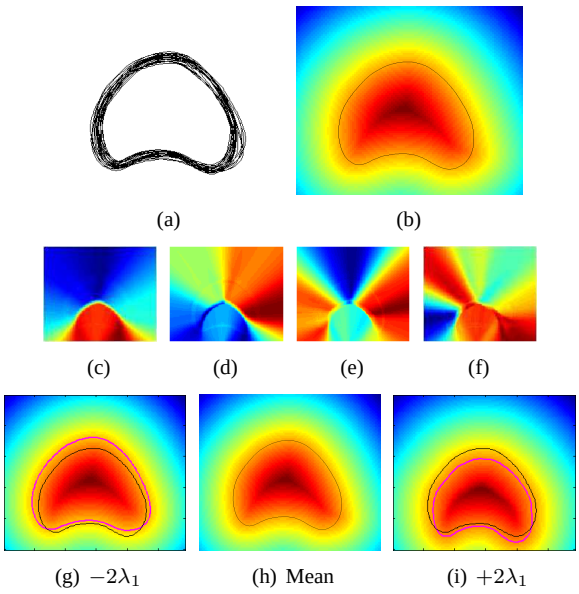

Figure 1. (a) The aligned contours of the training prostate images. (b) SDFs of the aligned training dataset with black contour showing the mean shape. (c), (d), (e), and (f) show the first four primary eigenmodes of variations of the prostate. (h) Shows the mean shape (black contour) $\overline{\Phi}$ and (g) and (i) represent the variance in mean shape (black contour) with $\overline{\Phi} \pm 2\lambda_1$ given by the magenta contour. From (b) to (i) red signifies high values and blue signifies low values.

2.2 Shape, region and contour based levelsets

The problem of segmenting the prostate using a shape prior, global and local image information could be resolved by minimizing,

$$F = F_{shape} + F_{region} + F_{boundary} \quad (1)$$

The process of building the shape model of the prostate starts with the alignment of n segmented prostate images of the training set with intensity based affine registration to minimize pose differences. The boundaries of each of the n aligned prostates are embedded as the zero levelset of n separate SDFs Ψ with negative distances assigned to the inside and positive distance assigned to the outside of the prostate boundary. The mean levelset function of the prostate is computed from the average of these n SDFs, $\overline{\Phi} = 1/n \sum_{i=1}^{n} \Psi_i$. To extract the shape variations of the prostates $\overline{\Phi}$ is subtracted from each of the n SDFs to create n mean-offset functions $\tilde{\Psi}$. Each 2D mean-offset $\tilde{\Psi}_i$ is reshaped into a column vector. Then the shape variability matrix of n prostates is given by $S = \left[\tilde{\psi}_1, \tilde{\psi}_2, ..., \tilde{\psi}_n\right]$. PCA of S yields the sorted matrix of principal components W_k (k is 98% of the total shape variations) and a vector of eigen coefficients x_{pca}. Hence the shape model is given as $\hat{\phi} = \overline{\Phi} + W_k x_{pca}$. The process of building the shape model is illustrated in Fig. 1. The energy associated

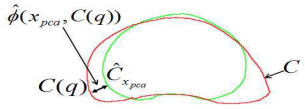

Figure 2. Illustration of shape function $\hat{\phi}(x_{pca}, C(q))$. The green contour gives the shape model and the red contour shows the evolving contour. The objective is to minimize the distance between the evolving contour and the shape model.

with the shape term may be given as,

$$F_{shape} = \oint_0^1 \hat{\phi}^2\left(x_{pca}, h_{x_T}\left(C\left(q\right)\right)\right)\left|C'\left(q\right)\right| dq \tag{2}$$

$$\hat{\phi}^2\left(x_{pca}, h_{x_T}\left(C\left(q\right)\right)\right) = \hat{\phi}^2\left(x_{pca}, C\left(q\right)\right) \approx \left|\hat{C}_{x_{pca}} - C\left(q\right)\right|^2$$

where C is the active contour at point q, x_{pca} is the vector of eigen coefficients and h_{x_T} is an element of a group of geometric transformation parameterized by x_T the geometric transformation matrix. This essentially evaluates the shape difference between the contour C and the zero levelset $\hat{C}$ of the shape function $\hat{\phi}$ as shown in Fig. 2. By minimizing this energy we restrict the levelset evolution to follow prostate shape prior. As discussed in 2.1 intensity of the image is substituted with posterior probabilities obtained with random forest. According to Chan and Vesse [3] MS functional model the curve parameters were determined from minimization of region based energy given by,

$$E_{cv} = \int_{R^u} (I-\kappa)^2 dA + \int_{R^v} (I-\gamma)^2 dA \tag{3}$$

Evolution of the curve ensured segmentation of the image into two region u and v with mean intensities κ and γ without any specific shape. In our model, the MS functional of [3] is modified to incorporate shape prior. The region based energy term as a function of the shape $\hat{\phi}$ is given as,

$$F_{region} = \int_\Omega \Theta_{in} H\left(\hat{\phi}\left(x_{pca}, x_T\right)\right) d\Omega + \int_\Omega \Theta_{out} H\left(-\hat{\phi}\left(x_{pca}, x_T\right)\right) d\Omega \tag{4}$$

where $H\left(.\right)$ is the Heaviside function and $\Theta_r = \left|I-\mu_r\right|^2 + \mu\left|\bigtriangledown \mu_r\right|^2$ and μ is the mean $r = in$ or out of the prostate shape prior. Gradient descent minimization of the energy term aids in determining the shape x_{pca} and the pose parameters x_T of the evolving curve to drive the shape model towards a homogeneous intensity region with the shape of interest. However, the model cannot handle local deformation like irregular boundaries of the prostate. Hence a new energy term is introduced as $F_{boundary}$ that aids in capturing the local edge variations around the global shape variations. Local edge information is captured by the energy term given as,

$$F_{boundary} = \oint_0^1 g\left(\left|\bigtriangledown I\left(C\left(q\right)\right)\right|\right)\left|C'\left(q\right)\right| dq \tag{5}$$

where $g\left(\cdot\right)$ is the Gaussian kernel applied on the image gradient (∇I). The energy minimization of F of Eq. (1) is performed using the gradient descent optimization.

Table 1. Prostate segmentation quantitative comparison (HD, and MAD in mm.) Statistically significant values are italicized

Method	DSC	HD	MAD
AAM [4]	0.94±0.03	4.92±0.96	2.15±0.94
Ghose [8]	0.95±0.02	3.82±0.88	1.26±0.51
Ghose [9]	0.96±0.01	2.80±0.86	0.80±0.24
Our Method	*0.97±0.01*	*1.73±0.24*	*0.42±0.09*

3. Experimental Results and Discussions

We have validated the accuracy and robustness of our method with 24 axial mid-gland TRUS images of the prostate with a resolution of 354×304 pixels from 6 prostate datasets in a leave-one-patient-out evaluation strategy. Manual segmentations performed by an expert radiologist were validated by an experienced urologist to prepare the ground truth. Both doctors have over 15 years of experience in dealing with prostate anatomy, prostate segmentation, and ultrasound guided biopsies. For the random forest based classification, we have fixed the number of trees to 100, the tree depth to 30 and the lower bound of information gain to 10^{-7}. These parameters were chosen empirically as they produced promising results with the test images. We have used most of the popular prostate segmentation evaluation metrics like DSC, 95% Hausdorff Distance (HD), and MAD, to evaluate our method. Furthermore, the results are compared with the traditional AAM [4], and to statistical shape and texture model of [8] and probability prior model of [9]. It is observed from Table 1 that a implicit representation of the evolving contour propagating on the probabilistic representation of the prostate regions in TRUS images significantly improves segmentation accuracy when compared to [4, 8, 9]. As opposed to the manual initialization of [4, 8], we use the posterior probability information for automatic initialization. We achieved a statistically significant improvement in t-test p-value <0.0001 in mean DSC, HD, and MAD compared to [4, 8, 9]. As observed in Table 1 better segmentation acuracies is achieved with texture features [8] and posterior probabilites [9] compared to the use of image intensities for curve evolution. However, use of posterior probability and implicit curve representation in our work provides better results when compared to [8, 9]. Working of our model and performance of different levelsets are illustrated in Fig. 3. To provide qualitative results of our method we present a subset of results in Fig. 4. The first row shows the results achieved with AAM [4] and the second row shows the results achieved with our method. A quantitative comparison of different prostate segmentation methodologies is difficult in absence of a public dataset and standardized evaluation metrics. Nevertheless, to have an overall qualitative es-

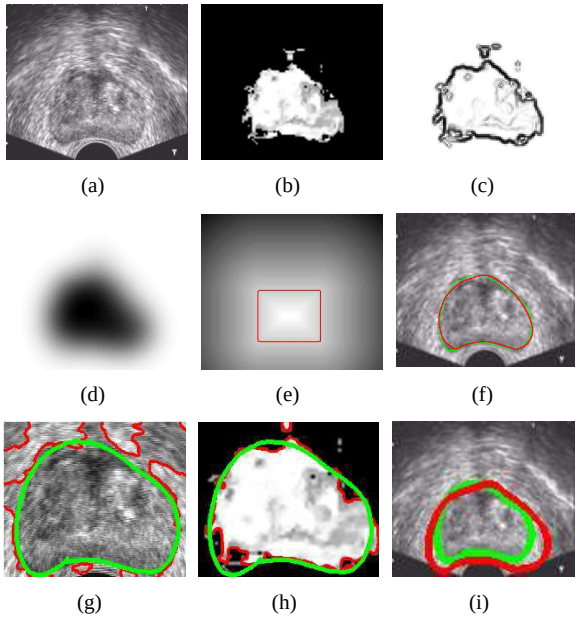

Figure 3. Illustration of working of our model and qualitative results of different levelsets. (a) is the image to be segmented, (b) random forest classification, (c) contour energy, (d) region based energy, (e) shows the initial levelsets (red contour) with SDFs and (f) segmentation with our model, (g) segmentation with levelsets [3], (h) segmentation with levelset [3] on posteriors, (i) segmentation with levelsets [1] on intensity. In (f), (g), (h), and (i) green contour is the ground truth and red contour is the obtained segmentation.

timate of the functioning of our method we have compared with some of the existing works in Table 2. Analyzing the results we observe that our mean DSC value is better compared to area overlap accuracy values of [11] and very similar to DSC value of [7]. However, it is to be noted that our MAD value is better compared to [11], [12], [5] and [7]. From these observations we may conclude that qualitatively our method performs well in overlap and contour accuracy measures.

4. Conclusions

A novel variational framework for curve evolution based on MS functional based on posterior probability information of the prostate region with the goal of segmenting the prostate in 2D TRUS images has been proposed. Our approach is accurate, and robust to significant shape, size and contrast variations in TRUS images when compared to traditional AAM and some of the works in literature.

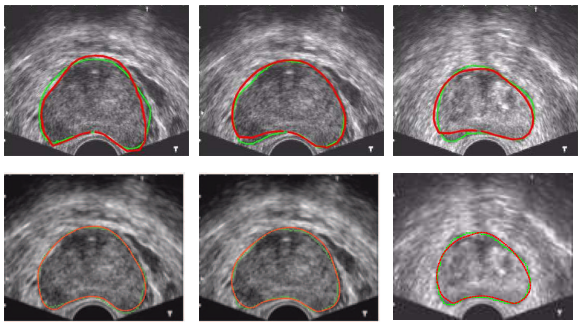

Figure 4. The green contour gives the ground truth and the red contour gives the obtained result. Row 1 shows the results achieved with AAM and row 2 shows results of our model for the corresponding prostates.

Table 2. Qualitative comparison of prostate segmentation; Ov=Overlap, Er=Error, Ac=Accuracy, Dt=Distance, px=pixels, mm=millimeter, Ds=datasets, im=images

Reference	Area Ac	Contour Ac	Ds
Shen [11]	Er 3.98±0.97%	Dt-3.2±0.87 px	8 im
Cosio [5]	-	MAD-1.6±0.6 mm	22 im
Yan [12]	-	MAD-2.10±1.02 mm	19 Ds/ 301 im
Ghose [7]	DSC 0.97±0.01	MAD-0.49±0.20 mm	23 Ds/ 46 im
Our Method	DSC 0.97±0.01	MAD-1.56±0.32 px/0.42±0.09 mm	6 Ds/ 24 im

References

[1] X. Bresson et al. A variational model for object segmentation using boundary information and shape prior driven by the Mumford-Shah functional. *Int. Jrnl. of Comp. Vision*, 68(2):145–162, 2006.

[2] L. Breiman. Random Forest. *Machine Learning*, 45(1):5–32, 2001.

[3] T. Chan et al. Active contours without edges. *IEEE Trans. on Imag. Proc.*, 10(2):266–277, 2001.

[4] T. Cootes et al. Active Appearance Models. *Eur. Conf. on Comp. Vision*, pages 484–498, 1998.

[5] F. A. Cosío. Automatic Initialization of an Active Shape Model of the Prostate. *Med. Imag. Analysis*, 12:469–483, 2008.

[6] L. M. Eri et al. Accuracy and repeatability of prostate volume measurements by transrectal ultrasound. *Prostate Cancer and Prostatic Diseases*, 5:273-278, 2002.

[7] S. Ghose et al. Multiple Mean Models of Statistical Shape and Probability Priors for Automatic Prostate Segmentation. *Prostate Cancer Imaging*, volume 6963 of *LNCS*, pages 35–46. Springer, 2011.

[8] S. Ghose et al. Statistical shape and texture model of quadrature phase information for prostate segmentation. *Int. Jrnl. of Comp. Assis. Rad. and Surgery*, 7:43–55, 2012.

[9] S. Ghose et al. A probabilistic framework for automatic prostate segmentation with a statistical model of shape and appearance. In *IEEE ICIP*, pages 713–716, 2011.

[10] D. Mumford et al. Optimal approximations of piece-wise smooth functions and associated variational problems. *Comm. on Pure & App. Mathematics*, 42:577–685, 1989.

[11] D. Shen et al. Segmentation of Prostate Boundaries from Ultrasound Images Using Statistical Shape Model. *IEEE Trans. on Med. Imaging*, 22:539–551, 2003.

[12] P. Yan et al. Discrete Deformable Model Guided by Partial Active Shape Model for TRUS Image Segmentation. *IEEE Trans. on Biomed. Engineering*, 57:1158–1166, 2010.